Light curve solutions of six eclipsing binaries at the lower limit of periods for W UMa stars

Diana P. Kjurkchieva[1], Dinko P. Dimitrov[2] and Sunay I. Ibryamov[1,2]

[1] Department of Physics, Shumen University, 115, Universitetska Str., 1712 Shumen, Bulgaria; *d.kyurkchieva@shu-bg.net*

[2] Institute of Astronomy and National Astronomical Observatory, Bulgarian Academy of Sciences, 72, Tsarigradsko Shose Blvd., 1784 Sofia, Bulgaria

Abstract Photometric observations are presented in *V* and *I* bands of six eclipsing binaries at the lower limit of the orbital periods for W UMa stars. Three of them are newly discovered eclipsing systems. The light curve solutions reveal that all short-period targets are contact or overcontact binaries and six new binaries are added to the family of short-period systems with estimated parameters. Four binaries have components that are equal in size and a mass ratio near 1. The phase variability shown by the *V-I* colors of all targets may be explained by lower temperatures on their back surfaces than those on their side surfaces. Five systems exhibit the O'Connell effect that can be modeled by cool spots on the side surfaces of their primary components. The light curves of V1067 Her in 2011 and 2012 are fitted by diametrically opposite spots. Applying the criteria for subdivision of W UMa stars to our targets leads to ambiguous results.

Key words: methods: data analysis — catalogs — stars: fundamental parameters — stars: binaries: eclipsing: individual (1SWASP J173828.46+111150.2, 1SWASP J174310.98+432709.6 ≡ V1067 Her, NSVS 11534299, NSVS 10971359, NSVS 11234970, NSVS 11504202)

1 INTRODUCTION

Most W UMa stars consist of solar-type components that have orbital periods within 0.25 d $< P <$ 0.7 d. They are recognized by continuous brightness variations and nearly equal minima. The short orbital periods of these binaries mean they have small orbits in which rotation is synchronized with revolution.

The statistics describing W UMa stars around the lower limit of their periods are quite poor (Terrell et al. 2012) because the period distribution of binaries reveals a very sharp decline below 0.27 days (Drake et al. 2014). Another reason is that these short-period binaries contain late-type stars and thus are faint objects that are difficult to study in detail.

However, short-period contact systems are important objects for modern astrophysics in at least two ways: (a) the empirical period-luminosity relation shown by W UMas allows one to use them as distance and population tracers; (b) these binaries are natural laboratories for the study of the late

Table 1 List of Our Targets

Target	Name	α_{2000}	δ_{2000}	Period [d]	V [mag]	ΔV	Ref
1	1SWASP J173828.46+111150.2	17 38 28.459	+11 11 50.05	0.249383	13.80	0.24	[1]
2	1SWASP J174310.98+432709.6	17 43 10.977	+43 27 09.48	0.258108	13.20	0.44	[2]
3	NSVS 11234970	19 32 07.875	+14 58 26.90	0.25074	13.66	0.63	[3]
4	NSVS 11504202	20 27 27.304	+12 30 50.66	0.24614	13.67	0.66	[3]
5	NSVS 11534299	20 48 20.859	+06 59 22.98	0.22465	13.40	0.21	[4]
6	NSVS 10971359	18 29 20.479	+07 58 07.26	0.27977	13.31	0.38	[3]

References: [1] Lohr et al. (2012); [2] Blattler & Diethelm (2000); [3] This paper; [4] Hoffman et al. (2009).

stage of stellar evolution connected with the processes of mass and angular momentum loss, merging or fusion of stars, etc.

Lately, interest in binaries around the low-period limit has increased because they provide constraints on theories describing the formation and evolution of low-mass stars. Moreover, one of the hypotheses for the origin of hot Jupiters is that they are products of a protoplanetary disk formed by the merging of short-period, low-mass binaries via "magnetic braking" if a substantial amount of mass remains in orbit around the primary (Martin et al. 2011).

Fortunately, modern large stellar surveys during the last decade have allowed the discovery of binaries with shorter and shorter periods (Rucinski 2007; Pribulla et al. 2009; Weldrake et al. 2004; Maceroni & Rucinski 1997; Dimitrov & Kjurkchieva 2010; Norton et al. 2011; Nefs et al. 2012; Davenport et al. 2013; Lohr et al. 2014; Qian et al. 2014; Drake et al. 2014). The majority of the newly discovered binaries from space missions (*Kepler, CoRoT*, etc.) and ground-based projects (ASAS, SuperWASP, Catalina, LINEAR, NSVS, etc.) have been classified as contact systems. However, most of them need follow-up observations and study.

In this paper we present photometric observations and light curve solutions for six binaries around the lower limit of orbital periods for W UMa stars. We chose to study such systems because the statistics of W UMa stars with periods around a quarter of a day are quite poor (Terrell et al. 2012). Three of our targets are known binaries: two binaries (1SWASP J173828.46+111150.2 and 1SWASP J174310.98+432709.6 ≡ V1067 Her) are from the SuperWASP photometric survey (Pollacco et al. 2006) and one system (NSVS 11534299) is from the NSVS database (Woźniak et al. 2004). Also, three of our targets (NSVS 11234970, NSVS 11504202 and NSVS 10971359) are newly discovered binaries. Table 1 presents the coordinates of our targets and information on their light variability.

The plan of the paper is as follows: Section 2 gives information for our observations and data reduction; Section 3 describes the procedure of the light curve solution of our data; Section 4 contains analysis of the obtained results; Section 5 gives subclassification of the targets; Section Conclusions summarizes the main results of the study.

2 OBSERVATIONS

The CCD photometry of the targets was carried out in 2011−2012 at Rozhen National Astronomical Observatory (Bulgaria) with the 60-cm Cassegrain telescope using the FLI PL09000 CCD camera (3056 × 3056 pixels, 12 μm pixel^{-1}, field of 17.1′× 17.1′). The average photometric precision per data point is 0.005 mag in I band and 0.008 mag in V band. Table 2 presents the journal of our simultaneous VI observations. In addition we obtained several observations in BVI colors of targets 1, 3 and 4.

The photometric data were reduced by the IDL software package (including subroutine DAOPHOT). We used more than three standard stars in the observed fields (Fig. 1). Table 3 presents their colors: I from the USNO-B1.0 catalog and V from the GSC 2.3.2 catalog. The magnitudes of the targets in Table 3 correspond to their out-of-eclipse levels from our observations.

Table 2 Journal of the Rozhen Photometric Observations

Target	Date	Filter	Exposure [s]	Phase range
1	2011 July 10	*V, I*	120,120	0.21–1.17
	2011 Aug 03	*V, I*	120,120	0.67–0.89
	2011 Aug 21	*V, I*	120,120	0.60–0.94
	2012 June 02	*V, I*	120,120	0.61–1.41
	2012 June 03	*V, I*	120,120	0.24–1.35
	2012 July 07	*V, I*	120,120	0.90–1.74
2	2011 Aug 11	*V, I*	120,120	0.20–1.08
	2011 Aug 19	*V, I*	120,120	0.83–1.74
	2012 June 04	*V, I*	120,120	0.86–1.33
	2012 July 08	*V, I*	120,120	0.35–1.38
3	2012 Aug 04	*V, I*	90,120	0.60–1.94
4	2012 Aug 05	*V, I*	120,120	0.63–1.91
5	2012 Aug 06	*V, I*	120,120	0.19–1.32
6	2011 July 08	*V, I*	120,120	0.45–1.24
	2011 July 11	*V, I*	120,120	0.16–0.90

Table 3 Magnitudes of the Targets and Their Standard Stars

Star	GSC-ID (USNO B1)	I [mag]	V [mag]	B [mag]
targ	1	12.21	13.46	14.68
st1	0100100125	11.55	12.67	13.41
st2	0100101007	10.83	12.20	13.62
st3	0099702419	11.04	12.49	14.15
st4	0099702343	11.10	12.57	14.09
st5	0099702387	11.85	13.12	14.10
targ	2	12.04	12.82	
st1	0310001679	12.49	13.00	
st2	0310001797	13.45	13.66	
st3	0310001604	11.13	12.01	
targ	3	12.45	13.66	14.33
st1	1049-0454686	12.88	13.44	13.87
st2	1049-0454529	10.91	12.45	13.33
st3	1049-0454842	11.75	12.88	13.41
targ	4	12.43	13.67	14.64
st1	0109500807	12.63	13.19	14.79
st2	0109501223	10.98	12.27	13.70
st3	0109500601	11.22	12.78	14.65
st4	0109501589	10.66	11.33	11.93
st5	0109500781	10.88	12.38	14.02
targ	5	11.97	13.19	
st1	0052402305	10.71	12.13	
st2	0052401323	11.50	11.93	
st3	0052401783	11.94	13.32	
targ	6	12.92	13.31	
st1	0102300733	12.14	12.34	
st2	0102302368	10.87	11.93	
st3	0979-0436284	13.77	13.97	

We also carried out a preliminary time-series analysis of our data using the software package *PerSea*. A comparison of the results with the published ones (Table 1) revealed two discrepancies.

(a) The published periods of targets 1 and 2 agreed well our data. However, the period of 0.24914 d for target 5 (see further Table 5) that we obtained was around 11% longer than the previous value (Table 1). This result is not so surprising because the follow-up observations of variable stars from different databases sometimes reveal different periods than the previous values (Norton et al. 2011;
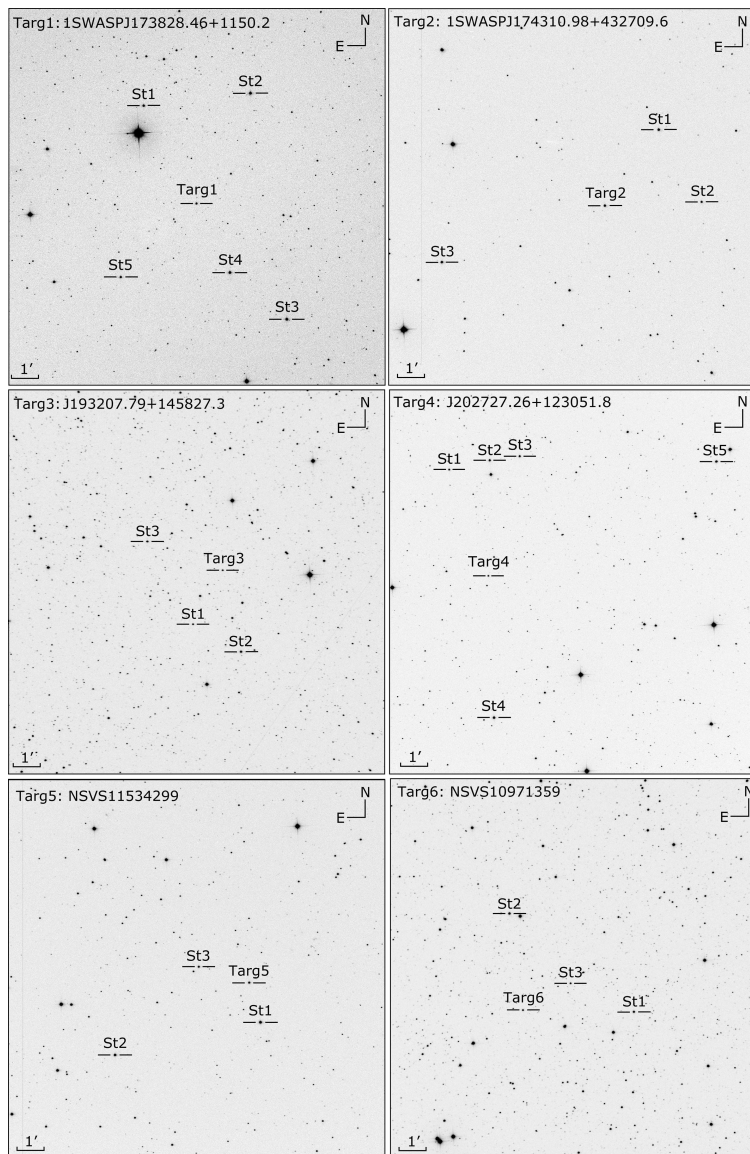
Fig. 1 The fields of the targets.

Mighell & Plavchan 2013; Lohr et al. 2013; Kjurkchieva et al. 2014; Mayangsari et al. 2014). This is a consequence of the automated frequency analyses of the huge data sets. They were based on different approaches, which turned out to have different precisions for different types of variabilities. Moreover, sometimes they gave several different periods for each target (as well as false alarm detections of exoplanets).

(b) The amplitudes of variability for targets 1 and 2 turned out to be considerably larger than the previous ones. We assume that the reason for this discrepancy is the low spatial resolution of the previous photometric observations by small telescopes (13.7″ pixel^{-1} for the SuperWASP survey and 14.4″ pixel^{-1} for NSVS) that can blur the separation of two neighboring stars. A close nonva-

Table 4 The 2MASS Color Indices J–K and Corresponding Mean Temperatures T_{m} for the Targets

Target	1	2	3	4	5	6
J–K	0.645 ± 0.033	0.590 ± 0.024	0.749 ± 0.030	0.750 ± 0.026	0.558 ± 0.034	0.618 ± 0.031
T_{m}	4720 ± 120	4930 ± 140	4320 ± 130	4320 ± 110	5090 ± 220	4810 ± 130

riable star may trigger a response from the same pixel during the photometric measurements of the variable star and thus reduce its amplitude of variability.

3 LIGHT CURVE SOLUTIONS

The shapes of the light curves (Figs. 2, 3, 4, 5, 6 and 7) implied that our targets are nearly contact or overcontact (OC) systems which was expected from their short orbital periods. The large amplitudes of their light variabilities mean that they are caused by eclipses.

It is well known that the determination of the mass ratio through the light-curve solution is an ambiguous approach compared with that by the radial velocity solution. However, the rapid rotation of components in short-period binaries is a serious obstacle to obtaining a precise spectral mass ratio from the measurement of their highly broadened and blended spectral lines (Bilir et al. 2005, Dall & Schmidtobreick 2005). On the other hand, their eclipse depths strongly depend on the potentials and the mass ratios.

Taking these considerations into account, we solved the Rozhen light curves of the six targets using the code *PHOEBE* (Prša & Zwitter 2005) by the following procedure.

We determined the mean temperatures T_{m} of the binaries (Table 4) by using their infrared color indices *(J–K)* from the 2MASS catalog and the color-temperature calibration of Tokunaga (2000).

At the first stage we adopted $T_1 = T_{\mathrm{m}}$ (a good approximation for contact binaries with close temperatures of the components) and searched for solutions with fixed T_1 by varying the initial epoch T_0, period P, secondary temperature T_2, orbital inclination i, mass ratio q and potential $\Omega_{1,2}$.

We adopted coefficients of gravity brightening $g_1 = g_2 = 0.32$ and reflection effect $A_1 = A_2 = 0.5$ appropriate for late-type stars while the limb-darkening coefficients for each component and each color were automatically updated to the stellar temperature according to the tables of van Hamme (1993).

In order to reproduce the O'Connell effect we added cool spots on the stellar surfaces and varied spot parameters (longitude λ, latitude β, angular size α and temperature factor κ). Moreover, the best fit in the two colors required a small contribution of third light l_3.

Finally, we searched for the best fits for fixed q, spot parameters and third light contributions by adjusting the primary temperature T_1 slightly above T_{m} and correspondingly changed T_2, $\Omega_{1,2}$ and i.

Table 5 displays the results of our light curve solutions. The parameter errors are the formal *PHOEBE* errors. The synthetic light curves corresponding to the parameters from Table 5 are shown in Figures 2, 3, 4, 5, 6, 7 and 8 as continuous lines.

The results of our light curve solutions can be used for estimation of the global parameters of the targets (masses, radii and luminosities) using statistical relations and the supposition that their components are approximate main sequence (MS) stars.

4 ANALYSIS OF THE RESULTS

The analysis of the light curve solutions led to several conclusions.

(1) All targets are almost contact ($\simeq$CB) or OC binaries. This result is expected taking into account the short periods of the binaries (Table 1).
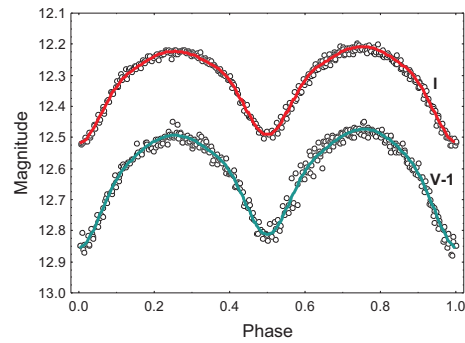
Fig. 2 Light curves of target 1 in V and I bands (the V data are shifted vertically by 1^m for better visibility) and their fits.
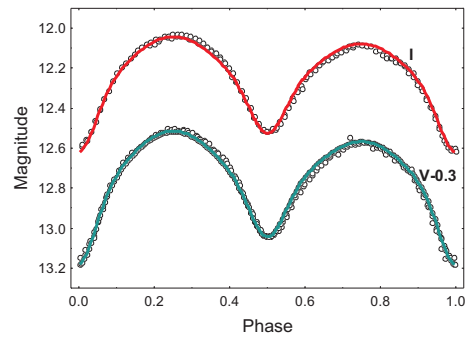
Fig. 3 Light curves of target 2 in V and I bands in 2011 (the V data are shifted vertically by 0.3^m for better visibility) and their fits.
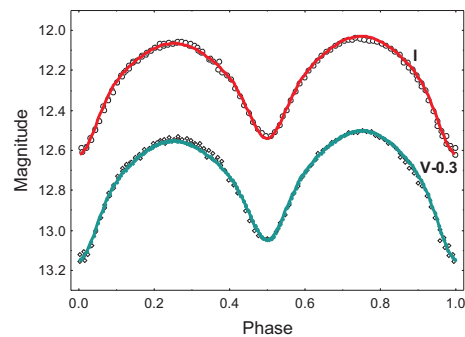
Fig. 4 Light curves of target 2 in V and I bands in 2012 (the V data are shifted vertically by 0.3^m for better visibility) and their fits.

(2) The q values are near 0.5 for two binaries (targets 1 and 6) and near 1 for the other ones. This result only refers to our sample and should be assumed to be accidental because the q values of W UMa stars are rather evenly distributed (fig. 1 in Csizmadia & Klagyivik 2004).

(3) The stellar components are K spectral type. This is a natural consequence of the average infrared colors of the targets (Table 4).
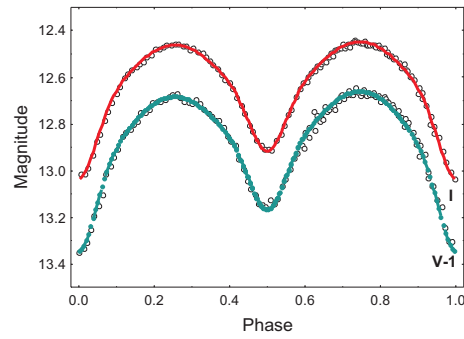
Fig. 5 Light curves of target 3 in V and I bands (the V data are shifted vertically by 1^{m} for better visibility) and their fits.
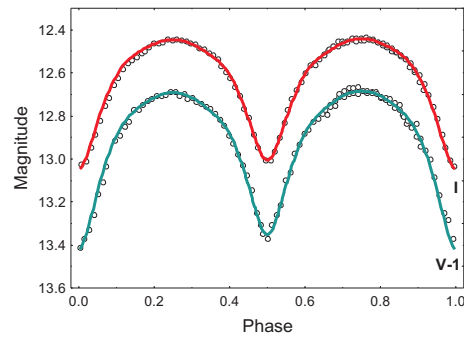
Fig. 6 Light curves of target 4 in V and I bands (the V data are shifted vertically by 1^{m} for better visibility) and their fits.
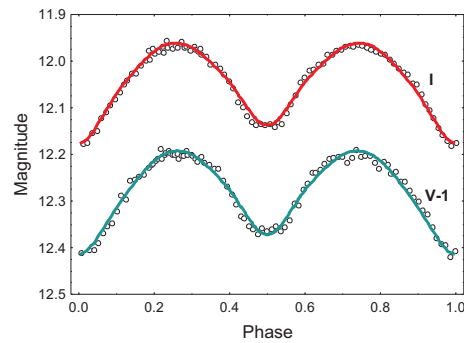
Fig. 7 Light curves of target 5 in V and I bands (the V data are shifted vertically by 1^{m} for better visibility) and their fits.

(4) The temperature differences in the components of the binaries are below 630 K. The small temperature differences are expected for contact or OC systems and mean that their components are almost in thermal contact.

(5) Four targets (2, 3, 4 and 5) have components that are equal in size, and they have a mass ratio near 1. Hence, their components obey the same mass-radius relation.
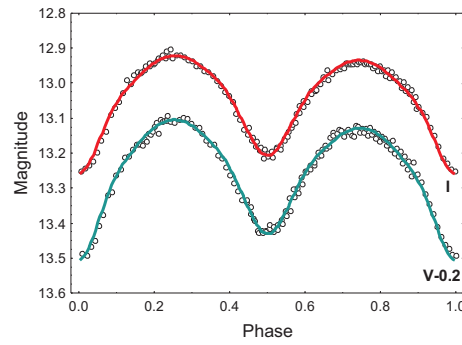
Fig. 8 Light curves of target 6 in V and I bands (the V data are shifted vertically by 0.2^{m} for better visibility) and their fits.

Table 5 Parameters of the Light Curve Solutions for the Targets

Parameter	1	2	3	4	5	6
T_0 2450000+	6091.94682	5785.294939	6144.364434	6145.36124	6146.46937	5751.49320
	±0.00021	±0.000151	±0.000208	±0.00011	±0.00021	±0.00021
P	0.249383	0.258108	0.25074	0.24614	0.24914	0.27977
			±0.00027	±0.00024	±0.00057	±0.00041
q	0.488 ± 0.002	1.009 ± 0.005	0.986 ± 0.006	0.980 ± 0.006	0.872 ± 0.003	0.462 ± 0.002
i	66.85 ± 0.09	75.68 ± 0.21	74.36 ± 0.26	79.4 ± 0.2	56.3 ± 0.4	66.8 ± 0.2
T_1	4900 ± 48	5152 ± 94	4600 ± 90	4402 ± 55	5150 ± 61	4936 ± 48
T_2	4544 ± 28	4626 ± 56	3969 ± 70	4219 ± 54	5014 ± 45	4423 ± 37
Ω_1	2.843 ± 0.004	3.640 ± 0.012	3.615 ± 0.009	3.717 ± 0.013	3.548 ± 0.014	2.785 ± 0.005
Ω_2	2.843 ± 0.004	3.640 ± 0.012	3.615 ± 0.009	3.717 ± 0.013	3.550 ± 0.008	2.785 ± 0.005
r_1	0.445	0.400	0.399	0.363	0.389	0.451
r_2	0.319	0.399	0.396	0.338	0.365	0.317
l_1	0.746	0.643	0.715	0.598	0.566	0.787
l_2	0.254	0.357	0.285	0.402	0.434	0.213
l_2/l_1	0.340	0.555	0.399	0.672	0.767	0.271
fillout	0.033	0.229	0.209	-0.045	-0.0024	0.061
fillout	0.033	0.229	0.209	-0.045	-0.003	0.061
configuration	OC	OC	OC	$\simeq$CB	$\simeq$CB	OC

Table 6 Parameters of the Cool Spots on the Targets

Target	β	λ	α	κ	l_3
1	122 ± 1	297 ± 1	17 ± 1	0.83 ± 0.01	0.029 (I)
2_{2011}	90 ± 1	90 ± 1	20 ± 1	0.80 ± 0.01	0.066 (I)
2_{2012}	90 ± 1	270 ± 1	20 ± 1	0.80 ± 0.01	0.034 (I)
3	90 ± 1	270 ± 1	18 ± 1	0.90 ± 0.01	0.055 (I)
4	90 ± 1	270 ± 1	10 ± 1	0.90 ± 0.01	0.085 (I)
5	40 ± 1	0 ± 1	20 ± 1	0.88 ± 0.01	0.073 (V)
6	90 ± 1	90 ± 1	15 ± 1	0.90 ± 0.01	0.057 (I)

(6) Five targets exhibited the O'Connell effect that could be modeled by cool spots (Table 6) on the side surfaces of their primary components. The light curves of target 2 in 2011 and 2012 were fitted by diametrically opposite spots (visible at the second and first quadratures correspondingly). This result can be explained by differential rotation or by a new spot cycle. However, the equal sizes and temperatures of the two spots (Table 6) rather support the first supposition.
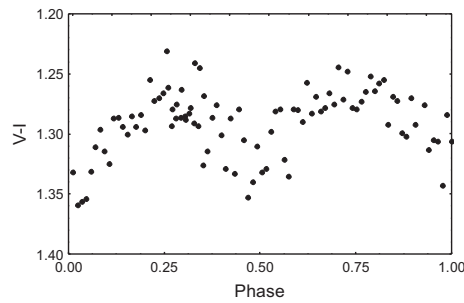
Fig. 9 $V - I$ light curve of target 1.

Table 7 Amplitudes of the Reddened (V–I) Colors and Amplitudes of I Variability for the Targets

Target	1	2	3	4	5	6
Δ (V–I)	0.06	0.08	0.10	0.14	0.03	0.07
ΔI	0.30	0.55	0.55	0.55	0.21	0.32

The modeling of the O'Connell effect in late-type stars by cool spots is the preferred approach by almost all authors. A cloud of circumstellar, absorbing matter that orbits the corresponding star may reproduce the O'Connell effect as a cool photospheric spot. However, only using photometric data (as is ordinarily the case) cannot resolve this ambiguity and one adopts modeling by spots.

(7) The cool spot on target 5 was invoked to reproduce the distortions in its light curve at the minima and maxima.

(8) The V–I indices of the targets undergo orbital variability with reddening at the light minima (Fig. 9). The amplitudes of the V–I curves are proportional to the light amplitudes (Table 7). This result means that the temperature on the back surface of the close stellar components is lower than those of their side surfaces.

(9) No target in our sample was identified as an X-ray source or H_α emission source. Thus, the low level of activity generally exhibited by W UMa stars was confirmed.

5 SUBCLASSIFICATION OF OUR TARGETS

The contact binary stars are divided into two subtypes, A and W, according to the following criteria: (a) the ratio R/T (radius to temperature): the larger star is the hotter one for an A subtype system while the smaller star is the hotter one for a W subtype system (Binnendijk 1970); (b) temperature T or spectral type: the A subtype systems are earlier than the W subtype binaries, whose components are G or K spectral type; (c) period P: the W subtype binaries have shorter periods of 0.22 to 0.4 days (Smith 1984); (d) mass ratio q: values for the A subtype are smaller than those for W subtype.

Csizmadia & Klagyivik (2004) introduced H subtype systems (H/A and H/W) with a large mass ratio ($q \geq 0.72$), whose energy transfer is less efficient than that in other types of contact binary stars. They found that the different subtypes of W UMas are located in different regions on the mass ratio – luminosity ratio diagram but above the line $\lambda = q^{4.6}$ ($\lambda = l_2/l_1$) representing the mass-luminosity relation for MS stars (fig. 1 in Csizmadia & Klagyivik 2004).

The subclassification of our targets according to the foregoing criteria is presented in Table 8. It reveals that almost all targets simultaneously belong to at least two subclasses. Only target 3 is deeply below the line representing the mass-luminosity relation for MS stars (the uninhabited place).

Table 8 Subclassification of the Targets

Criterion/target	1	2	3	4	5	6
T/R	A	A	A	A	A	A
T	W	W	W	W	W	W
P	W	W	W	W	W	W
q	A	W	W	W	W	A
$q, l_2/l_1$	A	H/A	?	H/A	H/W	A

This result means that the proposed criteria and subdivisions are ambiguous and, of course, that the stellar world is richer than one expects.

6 CONCLUSIONS

We obtain light curve solutions of six binaries with periods around 0.25 d, the lower limit of periods for W UMa stars. Three of the targets are newly discovered eclipsing systems.

The solutions reveal that all the systems are contact or OC binaries.

The colors of the investigated systems become redder at the light minima. Such a behavior may mean that the temperatures of the back surfaces of the close components are lower than those of their side surfaces.

The mass ratios of the targets are grouped around values 0.5 and 1 and those with a mass ratio near 1 have components that are equal in size.

Five targets exhibit the O'Connell effect that can be modeled by cool spots on the side surfaces of their primary components. The light curves of V1067 Her in 2011 and 2012 are fitted by diametrically opposite spots.

Applying the criteria for subclassification of W UMa stars to our targets leads to ambiguous results. New criteria are necessary for subclassifying the numerous W UMa systems.

This study adds six new systems with estimated parameters to the family of short-period binaries. They could help to improve statistics describing the relations between stellar parameters for low-mass stars.

References

Bilir, S., Karataş, Y., Demircan, O., & Eker, Z. 2005, MNRAS, 357, 497
Binnendijk, L. 1970, Vistas in Astronomy, 12, 217
Blattler, E., & Diethelm, R. 2000, Information Bulletin on Variable Stars, 4966, 1
Csizmadia, S., & Klagyivik, P. 2004, A&A, 426, 1001
Dall, T. H., & Schmidtobreick, L. 2005, A&A, 429, 625
Davenport, J. R. A., Becker, A. C., West, A. A., et al. 2013, ApJ, 764, 62
Dimitrov, D. P., & Kjurkchieva, D. P. 2010, MNRAS, 406, 2559

Drake, A. J., Djorgovski, S. G., García-Álvarez, D., et al. 2014, ApJ, 790, 157

Hoffman, D. I., Harrison, T. E., & McNamara, B. J. 2009, AJ, 138, 466

Kjurkchieva, D. P., Dimitrov, D. P., & Ibryamov, S. I. 2014, Information Bulletin on Variable Stars, 6113, 1

Lohr, M. E., Hodgkin, S. T., Norton, A. J., & Kolb, U. C. 2014, A&A, 563, A34

Lohr, M. E., Norton, A. J., Kolb, U. C., et al. 2012, A&A, 542, A124

Lohr, M. E., Norton, A. J., Kolb, U. C., et al. 2013, A&A, 549, A86

Maceroni, C., & Rucinski, S. M. 1997, PASP, 109, 782

Martin, E. L., Spruit, H. C., & Tata, R. 2011, A&A, 535, A50

Mayangsari, L., Priyatikanto, R., & Putra, M. 2014, in American Institute of Physics Conference Series, 1589, 37

Mighell, K. J., & Plavchan, P. 2013, AJ, 145, 148

Nefs, S. V., Birkby, J. L., Snellen, I. A. G., et al. 2012, MNRAS, 425, 950

Norton, A. J., Payne, S. G., Evans, T., et al. 2011, A&A, 528, A90

Pollacco, D. L., Skillen, I., Collier Cameron, A., et al. 2006, PASP, 118, 1407

Pribulla, T., Rucinski, S. M., DeBond, H., et al. 2009, AJ, 137, 3646

Prša, A., & Zwitter, T. 2005, ApJ, 628, 426

Qian, S.-B., Jiang, L.-Q., Zhu, L.-Y., et al. 2014, Contributions of the Astronomical Observatory Skalnate Pleso, 43, 290

Rucinski, S. M. 2007, MNRAS, 382, 393

Smith, R. C. 1984, QJRAS, 25, 405

Terrell, D., Gross, J., & Cooney, W. R. 2012, AJ, 143, 99

Tokunaga, A. T. 2000, Infrared Astronomy, in Allen's Astrophysical Quantities, ed. A. N. Cox (New York: AIP Press; Springer), 143

van Hamme, W. 1993, AJ, 106, 2096

Weldrake, D. T. F., Sackett, P. D., Bridges, T. J., & Freeman, K. C. 2004, AJ, 128, 736

Woźniak, P. R., Vestrand, W. T., Akerlof, C. W., et al. 2004, AJ, 127, 2436